Mismatch negativity results from bilateral asymmetric dipole sources in the frontal and temporal lobes.

Boutheina Jemel, Christiane Achenbach, Bernhard W. Müller, Bernd Röpcke and Robert D. Oades

University Clinic for Child and Adolescent Psychiatry and Psychotherapy, Essen, Germany

2002 Brain Topography, 15, 13-27

This is the reformatted manuscript submitted - prior to publication in its final form at (www.springerlink.com): doi:10.1023/A:1019944805499

Abstract:
The event-related potential (ERP) reflecting auditory change detection (mismatch negativity, MMN) registers automatic selective processing of a deviant sound with respect to a working memory template resulting from a series of standard sounds. Controversy remains whether MMN can be generated in the frontal as well as the temporal cortex. Our aim was to see if frontal as well as temporal lobe dipoles could explain MMN recorded after pitch-deviants (Pd-MMN) and duration deviants (Dd-MMN). EEG recordings were taken from 32 sites in 14 healthy subjects during a passive 3-tone oddball presented during a simple visual discrimination and an active auditory discrimination condition. Both conditions were repeated after one month. The Pd-MMN was larger, peaked earlier and correlated better between sessions than the Dd-MMN. Two dipoles in the auditory cortex and two in the frontal lobe (left cingulate and right inferior frontal cortex) were found to be similarly placed for Pd- and Dd-MMN, and were well replicated on retest. This study confirms interactions between activity generated in the frontal and auditory temporal cortices in automatic attention-like processes that resemble initial brain imaging reports of unconscious visual change detection.. The lack of interference between sessions shows that the situation is likely to be sensitive to treatment or illness effects on fronto-temporal interactions involving repeated measures.

Key Words:
attention auditory event-related potential dipoles frontal cortex, MMN, scalp current density temporal cortex, test-retest

Acknowledgements:
We are grateful for technical support from R. Franzka, J. Haverkorn, R. Windelschmitt and D. Zerbin. We also thank Professor C. Eggers for support. Some of the data were presented by Oades et al. at the 8th International Congress of Schizophrenia Research (Latebreaking Data), May 2001, Whistler, Canada.

Correspondence: **R. D. Oades,** University Clinic for Child and Adolescent Psychiatry and Psychotherapy, Virchowstr. 174, 45147 Essen, Germany.

INTRODUCTION

Mismatch negativity (MMN) is easily recorded in the scalp EEG response to a sound that deviates from the previous sequence or pattern of sounds heard. MMN is the negative-going difference obtained by subtraction of event-related potential (ERP) responses to standard sounds from those elicited by the deviants. To register this difference the mediating brain structures require at least 3-4 standards to set up a template (sensory memory) against which the deviance can be compared. A pause for 12-15 sec between stimuli usually results in the loss of this template (Cowan et al. 1993). Thus MMN reflects a form of short-term, auditory working memory (Näätänen 2000). It represents a largely automatic process for selecting and registering a stimulus as an MMN independent of the direction of the focus of attention. But, the size of the MMN does vary with the physical nature of the stimuli, and the state of consciously controlled attention (Oades and Dittmann-Balcar 1995; Tervaniemi et al. 2000).

This report addresses three major questions: a) where are the sources of MMN for auditory stimuli in both the frontal and temporal lobes, b) do these sources differ for two types of deviant (pitch and duration) and for two states (extra-modal visual vs. intra-modal auditory sustained attention), and c) are the features of the ERP component (amplitude and latency), topography and dipole-source (strength and latency) replicable over an interval of a month?

MMN is distributed topographically over fronto-central recording sites, but MMN dipoles that at least in part give rise to this distribution lie in the superior temporal auditory cortex (Sams et al. 1991; Scherg et al. 1989). Dipoles to auditory pitch- and duration-deviants may both have a similar diagonal orientation (contrast the dipole for intensity deviants), they may show more separation in the left than the right hemisphere (Giard et al. 1995), with that for the pitch-deviant lying more anterior, lateral and inferior to that for the duration-deviant (Frodl-Bauch et al. 1997). For about 10y there have been indications that activity centred in the frontal lobe could modulate temporal lobe sources, but clear evidence of a weak frontal current source was not published until 1998 (Deouell et al. 1998). While the general result, that there is a frontal MMN source, has been confirmed (Rinne et al. 2000), details about the location have not been published. Very recently Waberski et al. (2001) reported 3 temporal lobe sources and one in the midline cingulate. Using BESA rather than LORETA software we come to a different 4-dipole solution that proved stable for stimulus, condition and on re-test.

The need for (and the success of) replication of dipole characteristics and of component amplitude and scalp topography is important for the wide range of clinical applications for MMN records. MMN has been used to predict recovery from coma, the success of cochlear implant surgery, and to follow language development in children (review: Näätänen 2000). The MMN trace decays faster in Alzheimer's disease (Pekkonen et al. 1994), is very variable in alcoholics (Kathmann et al. 1995), declines in advanced age, but not in Parkinson's disease (Karayanidis et al. 1995): it is reduced in schizophrenia (Oades et al. 1996b; 1997; Javitt et al. 1998) and the topography changes in some types of schizophrenia, and in children with tics or ADHD (Oades et al. 1996a; 1997).

This study also addresses two questions to establish more firmly the basis for using MMN records in clinical studies of information processing following the effects of pre-/post-treatments or the course of an illness. First, how replicable are MMN waveforms following pitch *and* duration deviants according to amplitude, latency, morphology and topography as well as source? If the MMN amplitude elicited by one type of deviance is larger or has a simpler form, it would be preferable to use this stimulus-type when recording treatment effects. Indeed Giard et al. (1995) have already reported differences in latency, amplitude and form of MMNs resulting from intensity, pitch and duration deviants: separable topographic distributions within and between hemispheres and dipole orientations were also described. Such differences require replication and study.

The second question asks how similar are the MMN features on re-test? Test-retest coefficients for pitch-deviant dipoles were much better than those for duration-deviants (800/880Hz and 100/50 ms: Frodl-Bauch et al., 1997), yet this group later reported that the duration-deviant MMN amplitude prod-uced the more replicable form (Kathmann et al. 1999). Tervaniemi et al. (1999) using rapid presentations (300 ms intervals) also found better replicability for duration than pitch-deviant MMN, but commented that whether pitch or deviant was better varied between subjects. Indeed Deouell et al (1998) found pitch deviants far more reliable than using intensity, locus or stimulus intervals as a source of deviation. Using 700 vs. 600 Hz and 50 vs. 25 ms a similar degree of replicability was reported for pitch- and duration-deviants (r=0.58 vs. 0.67, Pekkonen et al. 1995) at 0.5 sec, but with poorer correlations at 1.5 sec inter-stimulus interval. Escera et al. (2000) also showed the potential importance of the inter-stimulus interval reporting modest correlations below 500 ms, but none at long 4 sec intervals.

In summary, we report on the nature of the MMN waveform, its dipole sources in the frontal and temporal lobes and the replicability of these results on re-test. As MMN may be considered a member of the family of N1 like components, the first section necessarily considers the features of the N1 in the current paradigm to demonstrate specificity.

MATERIALS AND METHODS

Subjects

Fourteen right-handed healthy adults (5 female, 21-36 years of age, mean 25 years) with normal hearing and normal or corrected-to-normal vision volunteered for the study. They attended to two recording sessions about 1 month apart. No participant had a history of neuro-logical or psychiatric illness and none used drugs affecting the central nervous system.

Stimuli

Visual and tone stimuli were generated with NeuroStim PC software. Sinusoidal tones (intensity: 76 dBspl) were presented binaurally (Dippacher TDH 39 earphones). Standard tones (Std: 82%) had a frequency of 1.0 kHz and lasted 80 ms, including 10-ms rise and fall times. Pitch-deviants (Pd: 6%) had the same duration but a higher frequency (1.5 kHz). Duration deviants (Dd: 6%) had the frequency of the standards but lasted 40 ms. Thus, the stimulus onset asynchrony (SOA) varied between 1040 and 1080 ms. Salient deviants were chosen to produce larger MMN amplitudes that produce more reliable test-retest sensitivity and larger signal-to-noise ratios for localisation analysis (e.g. larger MMN amplitudes for pitch-differences of 100 > 20 > 5% [Javitt et al., 1998] and for duration differences 50 > 25 ms [Joutsiniemi et al., 1998]). Complex novel sounds (6%, 80 ms long) were also presented but are not further considered in the present analysis. Visual stimuli consisted of red (50%) and green circles (50%). They were displayed in the centre of a computer screen, subtended an angle of 3.8° angle for the subject sitting 1.5 m away, and alternated every 1100 ms.

Procedure

In the 2 recording sessions (1 month apart) there were 2 conditions with 4 trial-blocks. Each block consisted of 400 tones (Std, Pd, Dd and Novel): the tones were presented in random order, except that each deviant was preceded by at least one standard tone. The 4 blocks of the passive condition were run in sequence, with a brief (ca. 1 minute) pause between each. After a longer pause (ca. 3 minutes) the 4 trial blocks of the active condition were run in a similar way. Each condition lasted ca. 13-15 minutes. The order of presentation of conditions was always the same to avoid the potentially confounding effect of Pd being a target before becoming a non-target. In the first passive auditory (attend-visual) condition, subjects were asked to ignore the tones and to look at a cross on the computer screen and to press a button in response to the green circle. The visual presentation represented a vigilance control. Conversely, in the active auditory condition (ignore visual stimuli) they were instructed to press a button upon detecting the rare pitch-deviants (Pd), to ignore the other tones, but to continue to fixate the circles on the computer screen. (Duration-deviant MMN was recorded here to control for state of attention (intra- *vs*. extra-modal). The onsets of the visual and auditory stimuli were controlled so they did not coincide. Within each condition the use of the left and right hand for key responses alternated between the four trial blocks. The procedure and the order of the experiments were the same in the two sessions.

ERP recordings

The EEG was recorded from 32 tin electrodes (Electrocap International) placed according to the international 10-20 system (Fz, Cz, Pz, Oz, F3, F4, C3, C4, P3, T3, T4, T5, T6 and at the left and right mastoids). The other sites were on the longitudinal axis (FCz, CPz) over the fronto-temporal (FT7, FT8), fronto-central (FC3, FC4), centro-parietal (CP4, CP3) and temporo-central regions (TP7, TP8). A vertical EOG was recorded from the supraorbital ridge and a horizontal EOG from the outer canthus of the right eye to monitor blink- and eye-movements. All sites were referenced to physically, closely balanced linked-earlobe electrodes. As the values for negative ERPs are large with earlobe reference they were used for purposes of representation and between-session correlations. The use of the nose- and the average-reference were

recomputed off-line for the purpose of topography and source analysis. The EEG signal (impedance < 5kOhm) was amplified using a SynAmp amplifier (Neuroscan, Herdon, VI) with a bandpass of 0.01–100 Hz, was digitised with 16-bit resolution, sampled at 500 Hz and stored on a hard disk. Artefacts (>50 μV) were removed automatically off-line. ERP data were collected separately for each tone type for 900 ms using a 100 ms pre-stimulus period for the baseline adjustment. The ERP was digitally filtered offline (30 Hz low-pass filter with 24-dB/octave attenuation) to eliminate high-frequency residual noise, and recalculated with respect to the average reference. Dipole computation was based on a time window (-50 to + 500 ms) and low-pass filtered to avoid aliasing (14 Hz, 24 dB/octave). (On analysis it was found that F4 had been incorrectly mounted and the data from this site had to be discarded).

Data analysis

This report considers two ERP components: a) the N1 in the stimulus-elicited waveform (peak negativity 80-140 ms at Fz and FCz), b) the MMN with a peak negativity between 100 and 200 ms (at Fz, FCz and Cz) in the deviant-minus-standard waveform (for the non-target Pd and Dd deviants in the passive condition and non-target Dd deviants in the active condition).

Statistical analyses were run separately for each of these components. N1 amplitude and latency were sub-mitted to a repeated-measure ANOVA, with tone (std, Pd, Dd), condition (passive *vs.* active), and electrode (Fz *vs*. FCz) as within subject factors. MMN waveforms in the passive condition were compared within subjects using a two-way ANOVA for midline sites for the factors deviant (Pd *vs*. Dd) and electrode (Fz, FCz, Cz), and a 3-way ANOVA for bilateral sites with deviant (Pd *vs*. Dd), laterality (left vs. right hemisphere), and electrode (F7-F8, FT7-FT8, FC3-FC4, C3-C4) as factors. A similar comparison was applied to the Dd MMN in the active condition. Test-retest reliability between sessions 1 and 2 for N1 and MMN used session as an additional factor in the ANOVAs. Pearson correlation coefficients were also calculated for between session measures. In the ANOVAs only the main effect of session and interactions involving the session factor were investigated. For all repeated measures with more than 1 degree of freedom, the conservative Greenhouse-Geisser adjusted F-values were used. Significant inter-actions were clarified by either breaking them into simple effects or by computing univariate *F* contrasts.

The use of topographic potentials for dipole calculations requires an independent reference. To eliminate error due to variations of potential to be expected from any single recording site (Nunez 1981) the average reference was used (Pasqual-Marqui and Lehmann 1993). Potential maps were computed with a spline interpolation algorithm, and the data presented as scalp current density maps (SCD: second spatial derivative of the potential) to enhance the focal sources (Pernier et al. 1988). This technique emphasizes local contributions to the surface map, providing a better visualization of the approximate locations of intracranial generators.

The sources of the electric potentials were modelled with Brain Electrical Source Analysis (BESA III, Scherg and Berg 1991). This program allows iterative fitting of the location and orientation of dipole sources in a head model until the difference between the recorded data and the calculated surface data of the dipole model is reduced to a minimum (least square fit). The source so modelled should be regarded as a potential centre of activity. It does not tightly constrain the calculated topography so that it is crucial to record accurately the fit of the modelled distribution occasioned by small changes of locus – the disparity being represent-ed by the unexplained variance. The goodness of fit is expressed by the residual variance (RV) as a percentage of the signal variance, which is minimised during the procedure. RV thus represents a measure of the model's quality. The model assumes a hypothetical spherical head (85 mm radius) and correction factors for the different conductivity of brain, skull, and scalp, treated as 3 shells (Scherg and Picton 1991). Each model was hypothesis led and first fitted to the ERP grand mean (session 1), that describes the most reliable characteristics of the spatio-temporal data

matrix and where the signal-to-noise ratio is better than in the individual traces. As a test of the stability of the dipole solution, the best models for each component were then applied to the individual subject data, and confirmed by fitting to the grand mean and the individual ERPs recorded in session 2. In summary, the modelling strategy following the a priori hypothesis (indicated by previously acquired data and/or SCD maps), takes account of the calculated vs. recorded waveform morphology, the unexplained variance in the grand mean and then the residual variance in the individual means. For each of the 2 conditions the individual ERP averaged data was based on a mean of more than 50 trials for each deviant and more than 640 trials for the standard tones.

To locate the sources neuro-anatomically the BESA dipole coordinates were transformed to those of the stereotaxic atlas of Talairach and Tournoux (1988) with software developed by Garnero, Baillet and Renault (1998: described in Crottaz-Herbette and Ragot 2000). Briefly the BESA sphere was centred on the posterior commissure (PC). The coronal coordinates were rescaled with linear transformations to match the anterior part of the sphere with the Talairach boxes anterior to the PC, and to match the posterior part of the sphere with the box posterior to the PC. Likewise the sagittal and axial coordinates were transformed according to the radius of the BESA sphere.

RESULTS

The N1 Component

Session 1, 2 and test-retest comparison

The N1 peaks had similar latencies after each tone (c.105 ms), were largest at Fz/FCz in both conditions, were reduced at temporal sites and absent at the mastoids (fig. 1). The smaller N1 after the Dd was followed by a second peak (c. 200 ms) in both conditions, at a delay that was longer than the stimulus duration.

After Pd the N1 peaks were twice as large as those after the standards and Dd tones in both conditions (F [1.6, 21.2] = 49.7, ε= 0.8, p < .0001) and sessions (F [1.1, 14.3] = 51.0, ε = 0.6, p < .0001). The only main effect of condition showed a larger N1 after Pd (not Dd) in the passive *vs*. the active condition of session 2. The tone x electrode interaction (session 1, F [1.6, 20.5] = 14.9, ε = 0.9, p < .0001) showed the standard N1 to be larger at FCz than Fz.

In both conditions and sessions, N1 peaked earlier after the standards (session 1, 100.7 ms $\pm$ 7.3: session 2; 100 ms $\pm$ 5.4) than the Pd- (109.4 ms $\pm$ 6.7 vs. 109.6 ms $\pm$ 9.5) and the Dd (112.3 ms $\pm$ 16.2 vs. 110.8 ms $\pm$ 19.0). The main effect of tone (not condition) was significant (F [1.1, 14.7] = 11.2/51.0, ε = 0.6, p < .004/.0001). The interactions were not significant.

The ERP waveforms (ear-lobe reference) for each tone showed similar morphologies and peak amplitudes between sessions (fig. 1): neither the main effect of session for N1 amplitude (F[1, 13] = 1.7, p = .2) nor latency (F[1, 13] = 3.6, p = .6) at Fz or FCz nor the two-way interactions with session were significant. Correlation coefficients were largest for Pd (both conditions) and standards (active condition): they were much lower for Dd (especially for amplitude) and lower in the passive vs. the active condition (especially for latencies: table I).

Session 1 and 2 topography and dipole source models

Reflecting a reversal of the polarity of the potentials, the SCD maps for each tone at the same latency showed a current sink (i.e., negative currents) bilaterally distributed over the fronto-central scalp, accompanied by bilateral posterior temporal current sources (i.e., positive currents) indicating generators in the left and right temporal cortices (data not shown). Analyses of the average-referenced fronto-central negativity confirmed those obtained with the ear-lobe reference showing

Table I.

Event-related Potential: Fronto-central midline sites: On the left side: On the right side

Components		*Fz*	*FCz*	*Cz*	*FC3*	*C3*	*FC4*	*C4*
N1 passive Pd	Ampl.	0.77**	0.92***					
Dd		0.60*	0.65*					
Std.		0.83**	0.82**					
N1 active Pd		0.94***	0.85***					
Dd		0.44	0.56*					
Std.		0.92***	0.92***					
N1 passive Pd	Lat.	0.69**	0.60*					
Dd		0.81***	0.76*					
Std.		0.25	0.07					
N1 active Pd		0.90***	0.89***					
Dd		0.85**	0.84**					
Std.		0.91***	0.92***					
N1 active	Ampl.	0.46	0.62*	0.68*	0.66*	0.70*	0.45	0.55*
	Lat.	0.75*	0.63*	0.56*	0.51	0.52	0.78**	0.74*
Pd-MMN	Ampl.	0.46	0.62*	0.68*	0.66*	0.70*	0.45	0.55*
	Lat.	0.75*	0.63*	0.56*	0.51	0.52	0.78**	0.74*
Dd-MMN passive	Ampl.	0.21	0.37	0.31	0.18	0.15	0.18	0.08
	Lat.	0.37	0.75*	0.78**	0.48	0.38	0.59*	0.11
Dd-MMN active	Ampl.	0.44	0.47	0.40	0.28	0.29	0.48	0.52
	Lat.	0.04	0.55*	0.52	0.12	0.38	0.11	0.14

Table I

Test-retest Pearson correlation coefficients for the amplitude and latency of the N1 in the passive and active condition for the three tones, the pitch-deviant (Pd-MMN, passive condition), and the duration-deviant (Dd-MMN, passive and active condition). ***p<0.0001; **p<0.001, *p<0.05

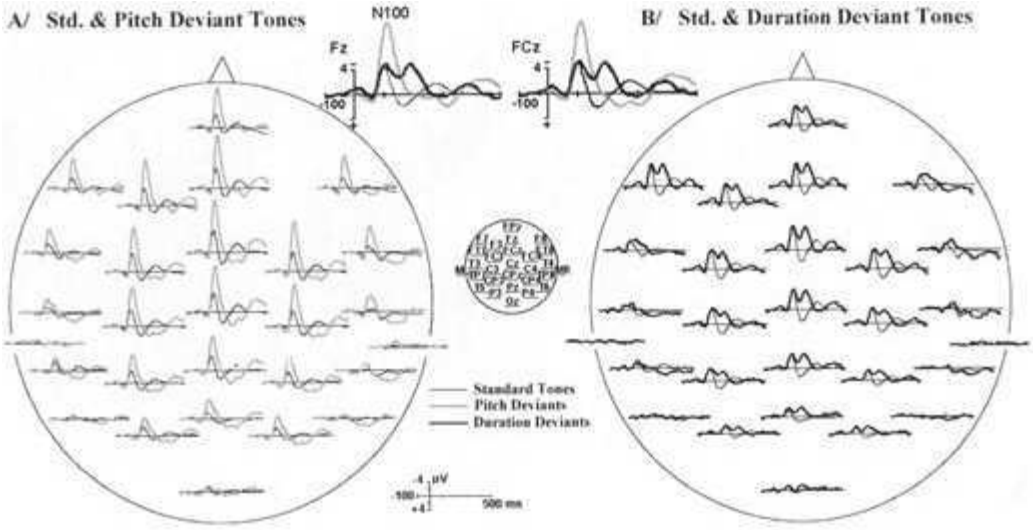

Figure 1

Session 1: passive condition: 28-site topography of ERPs elicited by A/ pitch-deviants (Pd) and standard tones (Std) [left], B/ duration deviants (Dd) and standards (Std.) [right], and at the top a close-up of waveforms after Pd, Dd and Std at Fz and FCz using a linked ear-lobe reference is shown. Note, the clear N1 peak at midline and lateral frontal sites and that compared to Pd, the Dd elicited a smaller, double peak

main effects of tone (F [1.2, 16.4] = 49.2, ε = 0.6, p < .0001), condition (F [1, 13] = 7.72, p < .02), and a tone x electrode interaction (F[(1.8,23.9] = 9.7, ε = 0.9, p < .001) in the absence of an effect of session. Similar analyses were obtained for the positive counterparts of N1, maximal at T5, T6 and mastoid sites.

To model the sources two symmetrical dipoles were placed initially in the centre of the head and the location and orientation adjusted to the time window of the N1 peak in the grand mean for each tone. Fitting the sources according to previous data (Fujiwara et al. 1998; Sams et al. 1991; Scherg et al., 1989) improved the explanation of the data with convergence on the temporal lobe. The translation in Talairach space confirmed sources for each tone in the superior temporal gyrus (STG). A better fit (reduced RV) was obtained for the deviants in the passive than in the active condition. The dipoles were deeper in the active condition (c. 15 mm, fig. 2). Application of the solution for session 1 to session 2 produced a similar or better RV with only minor adjustment to the orientation (passive/active conditions, Pd: 0.93% & 1.8%, Dd 2.99% & 4%, Std 2.49% & 2.8%; fig. 2). Thus, the N1 components elicited by the 3 tones showed slightly differently placed generators in the STG. These differences remained stable between sessions with no significant interactions between electrode, tone and session.

The Mismatch Negativity (MMN)

Session 1, 2 and the test-retest comparison

Fronto-central MMNs were recorded in the passive condition, with the Pd-MMN peaking more rostrally (Fz > FCz = Cz) than the Dd-MMN (FCz > Fz = Cz: tone X electrode, (F[1.2, 15.3] = 10.2, ε = 0.6, p < .001: fig. 3). In session 2 Pd-MMN proved larger than the Dd-MMN at these sites (F_s [1, 13] > 8.7, p_s < .013). This difference was stable between sessions (no effect of session or interaction with deviant, fig. 3). The positive-going MMN at temporal sites was larger for Pd than Dd in the passive condition on both sessions (F (1, 13) = 10.9, p < .006: fig.4, left). In part this may reflect some overlap with the N1 component.

Further in both sessions the Pd-MMN was more negative than the Dd-MMN over the right hemisphere (deviant x laterality interaction FC3-FC4 and C3-C4: F [1, 13] > 5, p_s < .045) and more positive over left temporal sites (F [1, 13] = 4.8, p < .05: fig. 4 left).

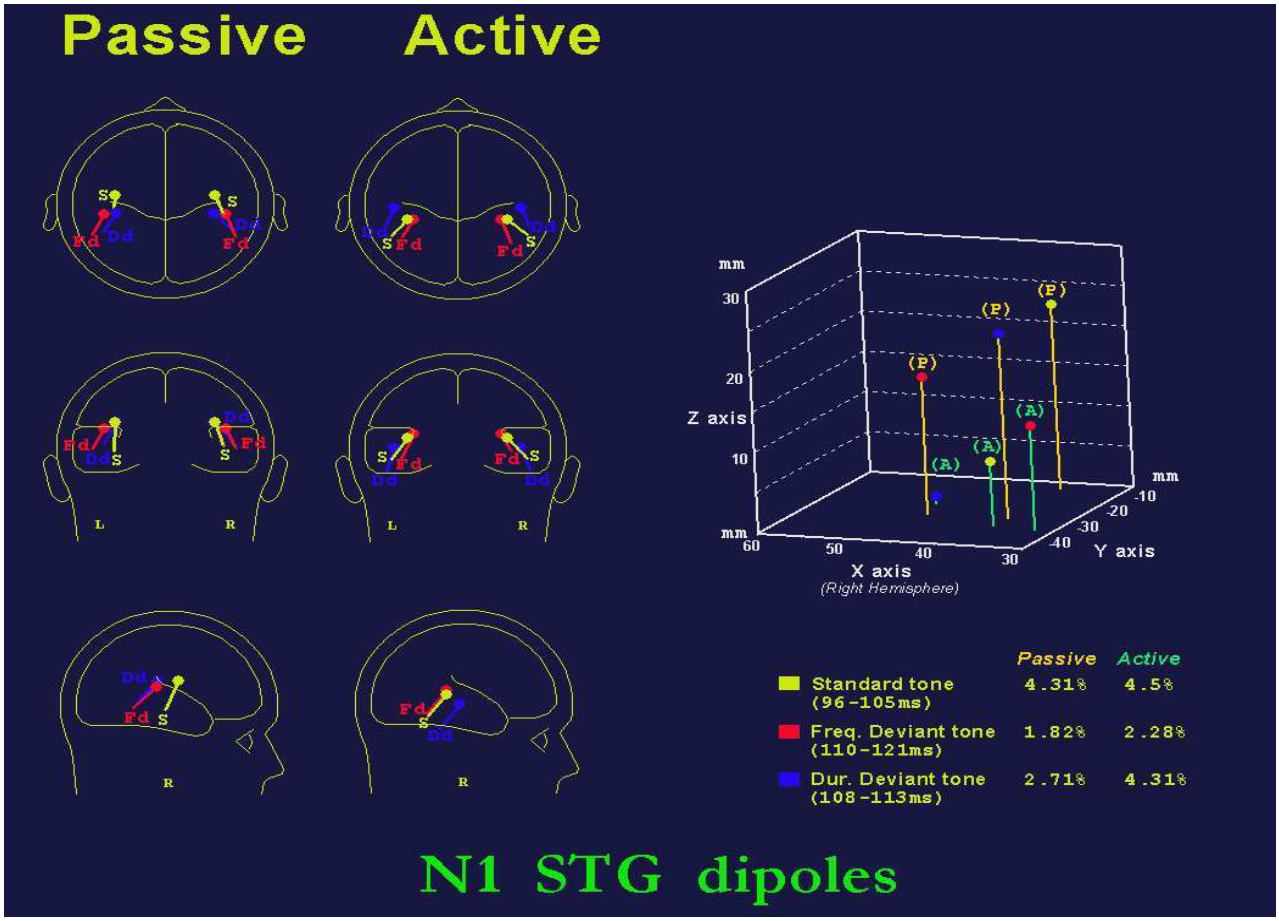

Figure 2
Spatio-temporal multiple dipole source analysis of the N1 component for the grand-mean ERP elicited by standards, pitch-- and duration-deviants in the passive (upper row) and active conditions (lower row). A symmetrical two dipole model is shown in a 4-shell spherical head model (BESA) with top, rear and lateral views of the head for each tone. On the right, the corresponding Talairach atlas locations of the dipoles in the right hemisphere are plotted in a 3D diagram (x-axis, sagittal; y-axis, coronal; z-axis, axial). Note the more superficial location of dipoles with lower residual variance values in the passive vs. the active condition.

In the active condition, with attention directed to the Pd tones, the amplitude of the Dd-MMN increased non-significantly (-5.8 μV ± 2.4 *vs*. -5.1 μV ± 2.6). Dd-MMN amplitude was smaller in session 2 *vs*. session 1 (F_s [1,13] > 4.88, p_s < .046), but this was not mirrored at temporal sites.

The Pd-MMN peak latency was about 20 ms later than for the N1, and 40 ms shorter than for the Dd-MMN (136.4 ± 31.1 vs. 184.7 ± 18.1 ms at Fz) at all fronto-central sites (F_s [1,13] > 69.9, p_s < .0001) in both sessions, reflecting the duration of the Dd tone. The Dd-MMN at fronto-central sites peaked non-significantly later in the active vs. passive condition (190 ms ± 26.1 *vs*. 181.2 ms ± 19.9).

The morphology and amplitudes of the grand mean MMN waveforms were very similar in both sessions (fig. 3). There were no significant differences between sessions for Pd-MMN and Dd-MMN amplitude at midline sites in either condition (main effect of Session: Pd-MMN F [1,13] = 2.6 p = .13; Dd-MMN passive/active: F[1,13] = 0.35/0.99, p = .56/.33, nor for bilateral comparisons (Pd-MMN: F[1,13] =3.64, p = .08; Dd-MMN passive/active: F[1,13] =0.006/ 3.3, p = .98/.092). Although no session x electrode interaction was significant for either MMN waveform in the passive condition, the Dd-MMN in the active condition showed a significant interaction over midline sites (F[1.3,16.3] = 10.71, ε = 0.6, p < .003) revealing a smaller MMN on session 2 *vs*. session 1 (Fz: F[1, 13] = 4.76, p < .05). Across sessions there were no significant latency

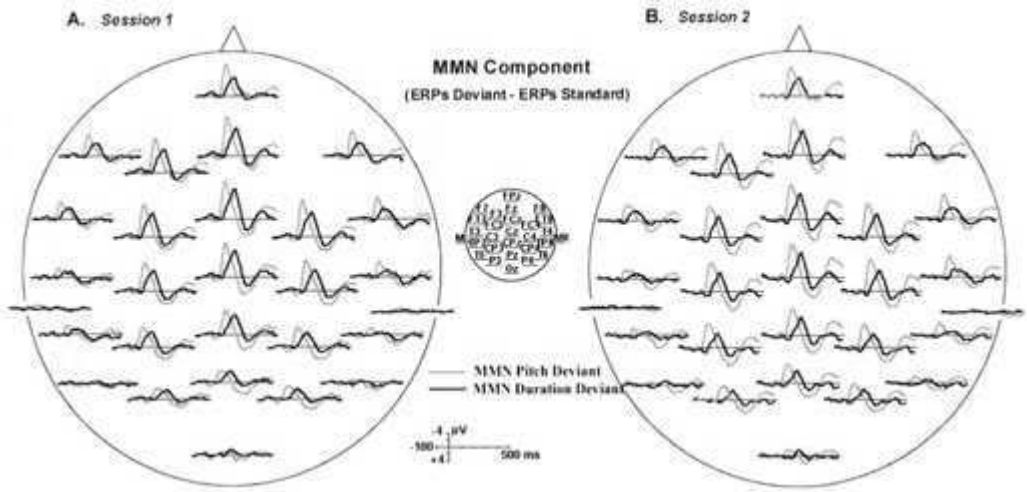

Figure 3
Session 1 (A, left) and 2 (B, right) 28-site topography of the grand-mean MMN waveforms (linked ear reference) for pitch-deviants (Pd, pale lines) and duration-deviants (Dd, black lines). Note the similar fronto-central distribution for both types of MMN on both sessions although the later Dd-MMN is smaller.

differences for the MMN after either deviant in either condition at any site (Pd-MMN: F_s [1, 13] < 1.1, p_s > .31; Dd-MMN passive/active: F_s [1,13] < 0.27/3.03, p_s > .61/.11) and no session x electrode interactions.

Pearson correlations for amplitude and latency between sessions were calculated for sites with clear MMN peaks (table I). Larger correlations for amplitude and latency measures were found for the Pd-MMN, but lower ones for Dd-MMN in the passive and active conditions.

Pd-MMN dipole source models (session 1 & 2)

MMN sources are reported with magnetoencephalography to be ca.10 mm rostral to the N1 source in the auditory cortex (Huotilainen et al. 1998; Korzyukov et al. 1999). Thus, models for the Pd N1 solution were explored first, with adjustments restricted to the 100-163 ms window. This 2-(bilateral)-dipole model provided a low RV (2%), but the waveforms they predicted did not adequately fit the potentials over frontal (Fz, F7-F8, FT7-FT8), left temporal and parietal sites. Therefore, two additional (bilateral) dipoles were added to explain the frontal activity, and the symmetry constraints were released. The location and orientation of these 4 dipoles explained the data very much better (RV = 0.87%) at all scalp sites (fig. 4a).

Matching this model to the activity from each subject required only minor optimising of the dipole orientation: (RV in 8 subjects 0.7-5.9%, in 4 subjects 7-10.8% and only 2 >10.8%). Use of this Pd-MMN 4-dipole solution in session 2 gave a similar fit to the grand mean data (RV 0.87%) and an even better fit to the individual data, (RV in 10 subjects 0.62-5.39%, in 3 subjects 6.32-7.99% and only one subject > 7.99%). Transformation into Talairach coordinates showed dipole 1 to be on the left temporo-parietal border (supramarginal gyrus), dipole 2 in the right STG, dipole 3 in the left cingulate gyrus, and dipole 4 in the right inferior frontal gyrus. The right temporal dipole peaked earlier (116 ms) than the cingulate (119 ms) and temporo-parietal dipoles (132 ms). The right frontal dipole was active later (157 ms: table II).

Dd-MMN dipole source models (session 1 & 2)

Initial models of the Dd-MMN source using the N1 solution in the 155-199 ms window gave a reasonable 2-dipole fit (RV 1.66%).

Table II: ***ERP Measures*** ***Dipoles*** ***Talairach Coordinates***

	Fz		Mastoids									
	Amplitude μV	latency ms	amplitude μV	latency ms	sources	F/T	BA	strength μV	latency ms	X	Y	Z
N1-*Std passive*	-2.5	105.6	2.1	100.1	1 left	T		6.9	99	-37	-14	+23
	(1.4)	(13.4)	(1.1)	(9.6)	2 right	T		11.3	102	+37	-14	+23
N1-*Pd passive*	-5.5	114.9	4.5	115.4	1 left	T		23.2	116	-46	-33	+17
	(2.5)	(8.3)	(2.4)	(7.2)	2 right	T		26.3	110	+46	-33	+17
N1-*Dd passive*	-2.9	120.7	2.2	114.2	1 left	T		10.7	113	-37	-33	+23
	(1.8)	(23.7)	(1.5)	(18.5)	2 right	T		11.9	108	+37	-33	+23
N1-*Std active*	-2.1	102.6	2.0	99.1	1 left	T		9.5	99	-37	-38	+ 8
	(1.5)	(15.3)	(1.1)	(8.4)	2 right	T		10.6	96	+37	-38	+ 8
N1-*Pd active*	-5.0	109.4	4.8	106.5	1 left	T		25.4	110	-32	-39	+13
	(2.0)	(8.4)	(2.5)	(10.0)	2 right	T		24.1	105	+32	-39	+13
N1-*Dd active*	-3.2	117.6	2.7	111.8	1 left	T		11.9	110	-47	-27	+ 1
	(1.9)	(24.0)	(1.5)	(18.0)	2 right	T		12.9	105	+47	-27	+ 1
MMN-*Pd*	-4.0	145.6	3.4	144.9	1 left	T	40	11.6	127	-44	-43	+32
	(1.3)	(35.7)	(1.7)	(30.5)	2 right	T	42	11.8	116	+53	-33	+15
					3 left	F	24 (post)	13.6	121	-17	-11	+41
					4 right	F	10/(46)/32	7.3	143	+44	+47	+ 9
MMN-*Dd*	-3.3	183.6	3.2	181.4	1 left	T	43	13.5	155	-38	-25	+32
	(1.6)	(29.2)	(2.2)	(24.1)	2 right	T	42	8.4	152	+55	-34	+15
					3 left	F	24 (post)	10.2	204	-17	-11	+41
					4 right	F	10/(46)/32	7.0	188	+38	+45	+ 2

Standard deviations in parentheses: Pd Pitch-deviant, Dd duration-deviant: Sources F, Frontal; T temporal lobe; BA Brodmann area

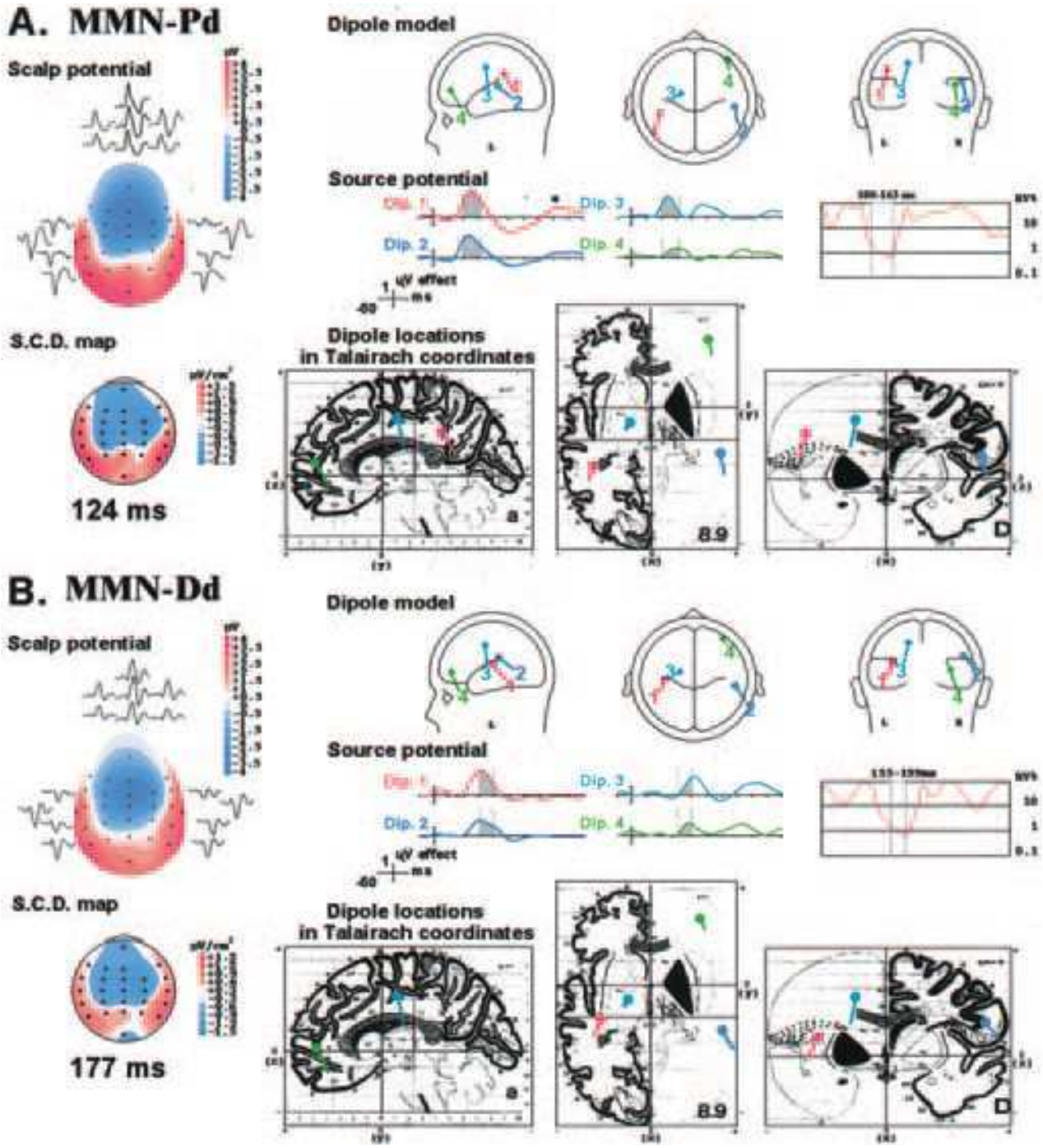

Figure 4
Topography and sources of MMN elicited by pitch- (A, Pd) and duration-deviants (B, Dd). *Left*. (A and B): Grand mean MMN across the scalp (average reference) and the comparable SCD maps. On the r*ight*, the 4-dipole spatio-temporal solution for Pd-MMN *(above)* and Dd-MMN *(below)*. *Upper row*, using a 4-shell spherical head model (BESA) views from the side, top and rear illustrate the locations of the dipole solutions. *Middle row*, strength of the source potentials for the 4 dipoles from -50 to 500 ms. The residual variance (RV) *on the right* is displayed on a logarithmic scale (ordinate) *vs*. time (abscissa) with a minimum at the MMN dipole latency. *Bottom row*, the location of the 4 dipoles in Talairach stereotaxic coordinates (x, sagittal, positive for the right side); y, coronal, positive rostral; z, axial, positive dorsal).

Adding frontal dipoles (as with the Pd above) improved the model (RV 1.06%), but only 3 dipoles were active in the modelled window, while the fourth remained inactive. Further, this solution did not successfully explain the individual data with RV > 6.04 % in 8 subjects on the first session

The alternative strategy, to apply the Pd-MMN dipole solution above, resulted in an RV of 0.85% for the 4 dipole solution. Thus, the MMN dipoles were located similarly for the Dd- and the Pd-tones on session 1 (fig. 4b). The RV for the grand mean data on session 2 increased to 2.36%, although the 4-dipole solution was stable between individuals and between sessions, (mean RV session 1, 8.1% $\pm$ 6.9; session 2, 5.9 $\pm$ 4.3: F[1,13] =1.1, ns). This model was significantly better than the previous one (F [1,13] = 11.1, p < .005). The Talairach coordinates placed dipole 1 in the left transverse temporal gyrus; dipole 2 on the right inferior parietal-STG border, dipole 3 in the left cingulate gyrus, and dipole 4 in the right inferior frontal gyrus. The posterior dipoles (1 and 2) were active earlier (at 149 and 152 ms) than the anterior ones (204 and 188 ms: table II).

DISCUSSION

Important, novel findings are the documentation of dipole sources for MMN in the frontal as well as in the auditory cortex, their stability between states of attention (intra- *vs*. extra-modal), their replicability between sessions, and their separation from sources for stimulus-elicited (N1) activity. The MMN sources proved similar if elicited by separate deviant features (pitch and duration), but pitch produced the better, more replicable measures.

Methods

We draw attention to the limits of our methods and how they were taken into consideration. First the design sought to demonstrate replicable N1 components with dipoles in the STG as a necessary basis for proceeding to analyse the later components that rely on this. Further it sought to demonstrate the similarity of MMN to two classes of deviant (Pd, Dd), and under the two states of intra- and extra-modal attention. The requirement of a replicable, quantitative baseline required for recording in 2 conditions and 2 sessions was met by the use of a simple vigilance task with response to one of two slowly alternating coloured circles. The same visual presentation in the auditory discrimination provided the perceptual balance and in the two sessions established the equivalence of vigilance states. This is an improvement on the frequent use of book-reading or video-watching in many other studies.

Dipole analysis and retest comparisons require good signal to noise ratios. Stimulus salience was assured by the 50% difference between standards and deviants. Under present conditions MMN amplitude would be expected to be 80-100% of maximum for pitch, duration, SOA and probability, and detectability was confirmed by the discrimination accuracy. Large amplitudes are achieved with moderately large physical differences (c. 50-150%), moderately low probability of occurrence (3-12%) and moderately long inter-stimulus intervals (500-1000 ms). Above and below these values an attenuation of amplitude can be expected (Javitt et al. 1998; Joutsiniemi et al. 1998; Shelley et al. 1999; Michie et al. 2000 and references therein). Signal to noise ratios are also important for source analysis. Preliminary inspection of topographic potential maps was improved by radial SCD maps obtained by computing spatial derivatives of the spline functions used in potential map interpolation. These maps, based on >50 sweeps/ deviant/condition, are reference free, and show sharper peaks and troughs. This facilitates the interpretation of overlapping sources that could potentially arise in the STG (Pernier et al. 1988; Alcaini et al. 1995). These maps provide the starting point for modelling, and thus have an advantage over magnetoencephalographic techniques that are sensitive to superficial not deep, and to tangential not radial dipoles. Hence studies of frontal contributions to MMN necessarily depend on electrophysiological measures (Rinne et al. 2000).

Laarne et al (2000) recently com-pared the

accuracy with which they could model real dipoles with 19 to 64 sites under variations of input noise that can arise from variations in brain/scalp resistivity (160-200 vs. 60-80 Ohm-metres). With the deepest dipole and greatest noise (worst case) they found that resolution deteriorated from 1 to 2 cm. Yvert et al. (1997) simulated data in 4 different spherical models for 19, 32 and 64 electrodes and reported error varying for 32 sites from ca 3 mm at the surface to 12 mm at deep sites. Thus we posit that the error in our coordinates would not greatly exceed c.10 mm. (This compares with a resolution of about 3-6 mm attributed to haemodynamic methods [Cabeza and Nyberg 2000]). Given that these studies did not find significantly improved resolution with 64 electrodes, the direction for improvement would lie in the digital integration of electrode location with head land-marks for each individual, and localising these on individual MRI anatomical images.

Test-retest replicability:

The highly significant intra-individual stability over a month for N1 amplitude and latency after each tone replicates earlier studies (Pekkonen et al. 1995 and references cited). Lower correlations in the Dd waveform may reflect variation in the two-peak morphology arising from stimulus-offset at 40 and 80 ms. MMN correlation coefficients were lower than for N1, but larger for the Pd- than the Dd-MMN, or those reported by Pekkonen et al. (1995). Slightly better correlations were achieved with SOAs shorter than 1 sec (Pekkonen et al.1995; Escera et al. 2000), but in view of the 2-peak Dd morphology it is not surprising that Escera et al. achieved slightly better values using a window measure for amplitude. Nonetheless, as here, Escera et al. reported better correlations for the Pd-MMN than Kathmann et al. (1999), whose results are difficult to reconcile with their earlier report of more reliable results for the Pd than Dd dipole (Frodl-Bauch et al. 1997). Poorer correlations reported by Tervaniemi et al. (1999) for Pd *vs.* Dd deviants may be explained by salience differences (Dd differed by 50% while pooled pitch deviance varied 5-10%). The test-retest correlations for Pd-MMN amplitude and dipole measures (with averaged and linked-ear-referenced data) compare with those of Escera et al. (2000). Modest test-retest correlations for MMN peak latency imply that the design may not accurately demonstrate differences in information processing speed.

N1 Component

N1 amplitudes were sensitive to stimulus features (Pd > Dd ≅ standard) and slightly larger in the discrimination condition. In both conditions the dipole strength for Pd was double that for the Dd. Our data accord with a tonotopic distribution of sources within the auditory cortex (Giard et al. 1995). Latencies were longer after deviants. These features were mirrored in positive peaks at mastoid sites. The dipole locations are quite similar to fMRI activity elicited by the oddball task (e.g. novelty/non-target comparisons, Kiehl et al. 2001) if more superficial (see also Alho et al. 1998b). But the deeper dipoles in the active condition approach those reported by Kiehl et al. for target comparisons. Comparisons with other dipole studies are difficult as they do not report coordinates, but small variations are likely de-pending on which of the N1 subcomponents dominated, which is in turn is sensitive to SOA (Teale et al. 2000).

Mismatch Negativity (MMN)

Latency: The peak latency for the Pd-MMN at 136 ms occurred 49 ms earlier than that for the Dd-MMN. This reflects the 40 ms shorter duration of the Dd tone where the offset marks the deviance. Clearly, the use of Dd incurs risks of interpretation if the length of the stimulus is not integral to the study. Independent of tone or condition, the frontal MMN dipoles peaked up to 40 ms later than those in the temporal cortex. Recently, Rinne et al.(2000) described possible frontal MMN sources for spectrally rich tones based on SCD maps, and also suggested that they peaked later, albeit by only 8 ms. Both studies found the significant difference in the right hemisphere. On the assumption that the frontal source controls the switch between stimuli previously registered in the temporal

cortex this latency difference may be crucial to the role of the frontal dipole in (involuntary) switching attention to a sound change. Arguably less crucial is an emphasis on the role of the right hemisphere, firstly because we found that the latency difference could be zero for the left hemisphere, and secondly Rinne et al. reported the mirror image of this delay on the left for some subjects.

A*mplitude and Sources:* The Pd-MMN amplitude was c.20% larger than that for the Dd-MMN (see discussion above). The good replicability and large phase reversal at mastoid sites lends credence to the usefulness of the stimulus parameters chosen. The influence of focussing attention on the auditory modality over ignoring it, in the presence of a visual control for diffuse attention, incurred an increase of 13-14% in the Dd-MMN. Although the effect was not significant it is consistent with previous reports of increased MMN under conditions of directed attention (Alain and Woods 1997; Oades and Dittmann-Balcar 1995) and imaging studies of fronto-temporal interactions in auditory attention (Alho et al. 1999).

The Pd-MMN, unlike the Dd-MMN, was more marked over the right hemisphere. While a right predominance has been noted for MMN based on other sorts of stimuli (Paavilainen et al. 1991), it is more consistently reported for Pd-MMN (Alain et al. 1998; Deouell et al. 1998; Levänen et al. 1996; Otten et al. 2000). Undoubtedly this lateralization must partially reflect the nature of the stimulus, but also the brain specialisation in development. Speech-like stimuli induce an MMN in infants (and adults) that is larger on the left (Alho et al. 1998a; Dehaene-Lambertz and Baillet 1998). Neuroimaging studies confirm this left lateralization for speech-like stimuli, but static or slowly changing frequencies activate the right side (Müller et al. 2001). Consistent with this Pd-MMN develops on the right at 10 years in healthy children, while in those with ADHD, that reflects developmental impairments of attention, it is seen first on the left (Oades et al. 1996a). Situations that require sustained attention activate preferentially cerebral blood flow in the right hemisphere (Paus et al. 1997). But relevant to an interpretation of the MMN function, with frontal lobe involvement, it should be noted that Nobre et al. (1999) reported right frontal blood flow activation during breaches of expectation (i.e. deviance) in performing tests of the covert orienting of attention.

Ten years ago 2 MMN sources were reported in the superior temporal plane of primary and secondary auditory cortices rostral to the principle N1 generator (Paavilainen et al.1991; Sams et al. 1991; Scherg et al. 1989). A degree of tonotopic ordering was described but with N1 sagittally displaced to the primary region in Heschl's gyrus and the MMN in the anteromedial secondary areas (Cansino et al. 1994; Csepe et al. 1992; Tiitinen et al. 1993). Giard et al. (1990, 1995) suggested the potential of frontal lobe activity to modulate their strength. Studies of patients with frontal, parietal and temporal lobe damage showed that MMN was reduced ipsilateral to the insult and more so on the right (Alho et al. 1994; Woods et al. 1994). Some looked for and did not find a frontal dipole (Frodl-Bauch et al. 1997), others found hints of a right parietal source (Deouell et al. 1998; Levänen et al.1996). Reports of at least one frontal source are recent (Deouell et al 1998; Jemel et al. 2001; Waberski et al. 2001).

The locations of the dipoles for Pd-MMN and Dd-MMN in the STG were remarkably similar, although the latter appeared slightly more posterior on the left side. On the right these loci are in BA 42 and on the left they are in Heschl's gyrus close to the border of the supra-marginal gyrus (BA 40). Frontal sites on the right were located in the inferior frontal gyrus between the middle frontal and anterior cingulate gyri (BA10/24). On the left the dipoles are in the posterior part of the anterior cingulate region (BA 24) at the rostro-caudal level of the post-central-parietal border (cf. reports on parietal sources, cited above).

The dipole locations in the STG are remarkably similar to fMRI activity elicited by deviant and unattended novel sounds (Opitz et al. 1999a, b), if marginally more medial

(Yoshiura et al. 1999) and superficial (Kiehl et al. 2001) than activity elicited by the oddball task But we cannot confirm that MMN sources are necessarily anterior to those for the N1 (Tiitinen et al. 1993, see discussion above). For the frontal sources there is qualified support from fMRI reports of increased activity in non-target comparisons from several regions. Superficially striking is the similarity of the MMN locus in the right hemisphere with activity in the right inferior frontal gyrus after auditory stimuli (Kiehl et al. 2000; review Müller et al. 2001) and a generic "deviance detection system" for oddballs independent of stimulus attributes (Strange et al. 2000). Indeed Beck et al. (2001) also reported right inferior frontal activity associated with consciously undetected visual change. However, both these loci appear to be some 10 mm postero-dorsal to the one described here. Similarly Kiehl et al report activity in the left cingulate as here, but about 10 mm more antero-ventral.

Anatomical Considerations: temporo-frontal connections

The temporal lobe sources match published coordinates for Heschl's gyrus and the area of the circular sulcus quite well (Leonard et al. 1998: e.g. features associated with Heschl's gyrus, on the left at x=38, extend y=-26 to –43 and z=4 to 17; while at x=48, they extend y=-12 to –44 and z=2 to16). Thus N1 sources that were deeper and more posterior in the active condition still remained within the gyrus. This is analogous to visual stimuli, where focussed attention effects were recorded in association not primary visual cortex (Hillyard et al. 1997).

The primary auditory cortex in the superior temporal plane is surrounded by secondary association areas in the circular sulcus and STG. From here Pandya (1995) described three lines of frontal projections: a more medial limbic (root line), in the STG (a belt line) and interposed a core line. The first two regions have long association connections with medial prefrontal (and orbitofrontal) regions while the third set of associations project to more caudal frontal regions. These are consistent with the differential more polar and more caudal dipole sources described. The differential pathways may reflect differential functions. Mesulam (1998) suggested that the more dorsal STG detects sounds and their spatial localisation, whereas the more ventral areas (here prominent in the active session) are involved in identification processes such as in auditory sequences. Considering the polar location of the frontal dipole in BA9/10 it should be emphasised that these connections have been shown to be reciprocal (Barbas et al. 1999) and the reciprocal connection is active in focussed attention (Rempel-Clower and Barbas 2000).

Conclusions:

We report good test-retest reliability for pitch-deviant N1, and MMN peaks and their dipoles recorded over a month apart under conditions suitable for measuring *both* indices of automatic and controlled processing (e.g. moderately long SOA). Dd-MMN and MMN latencies were replicated more modestly. Thus this paradigm provides a good starting point for monitoring potential pre-post alterations resulting from operations or illness treatments where automatic or controlled selective information processing may be affected.

Distinct sources for the N1, and MMN components were described in the STG. Change detection elicited localised frontal activity, with the more polar source in the right inferior frontal cortex, consistent with automatic stimulus processing. The contralateral source was in the cingulate.

REFERENCES

Alain, C. and Woods, D.L. 1997. Attention modulates auditory pattern memory as indexed by event-related potentials. Psychophysiology, 1997, 34: 534-546.

Alain, C., Hargrave, R. and Woods, D.L. Processing of auditory stimuli during visual attention inpatients with schizophrenia. Biol. Psychiatry, 1998, 44: 151-1159.

Alcaini, M., Giard, M-H., Echallier, J-F. and Pernier, J.F. Selective auditory attention effects in tonotopically organized cortical areas: a topographic ERP study. Human

Brain Mapping, 1995, 2: 159-169.

Alho, K., Woods, D.L., Algazi, A., Knight, R.T. and Näätänen, R. Lesions of the frontal cortex diminish the auditory mismatch negativity. Electroencephalogr. Clin. Neurophysiol. 1994, 91: 353-362.

Alho, K., Connolly, J.F., Choeur, M., Lehtokoski, A., Huotilainen,M., Virtanen, J., Aulanko, R. and Ilmoniemi, R.J. 1998a. Hemispheric lateralization in preattentive processing of speech sounds. Neurosci. Lett., 1998a, 258 :9-12.

Alho, K., Winkler, I., Escera, C., Huotilainen, M., Virtanen, J., Jääseläinen, I.P., Pekkonen, E. and Ilmoniemi, R.J. Processing of novel sounds and frequency changes in the human auditory cortex: magneto-encephalographic recordings. Psycho-physiology, 1998b, 35: 211-224.

Alho, K., Medvedev, S.V., Pakhomov, S.V., Roudas, M.S., Tervaniemi, M., Reinikainen, K., Zeffiro, T. and Näätänen, R. Selective tuning of the left and right auditory cortices during spatially directed attention. Cog. Brain Res., 1999, 7: 335-341.

Barbas, H., Ghashghael, H., Dombrowski, S.M. and Rempel-Clower, N.L. Medial prefrontal cortices are unified by common connections with superior temporal cortices and distinguished by input from memory-related areas in the Rhesus monkey. J. Comp. Neurol., 1999, 410: 343-367.

Beck, D.M., Rees, G., Frith, C.D., and Lavie, N. Neural correlates of change detection and change blindness. Nature Neurosci., 2001, 4: 645-650.

Cabeza, R. and Nyberg, L. Imaging cognition II: an empirical review of 275 PET and fMRI studies. J. Cogn. Neurosci. 2000, 12: 1-47.

Cansino, S., Williamson, S.J. and Karron, D. Tonotopic organization of human auditory association cortex. Brain Res., 1994, 663: 38-50.

Cowan, N., Winkler, I., Teder, W. and Näätänen, R. Memory prerequisites of mismatch negativity in the auditory event-related potential (ERO). J. Exp. Psychol. Learn. Mem. Cog. 1993, 19: 909-921.

Crottaz-Herbette, S. and Ragot, R. Perception of complex sounds: N1 latency codes pitch and topography codes spectra. Electroencephalogr. Clin. Neurophysiol., 2000, 111: 1759-1766.

Csepe, V., Pantev, C., Hoke, M., Hampson, S. and Ross B. Evoked magnetic responses of the human auditory cortex to minor pitch changes: localisation of the mismatch field. Electroencephalogr. Clin. Neurophysiol., 1992, 84: 538-548.

Dehaene-Lambertz, G. and Baillet, G. A phonological representation in the infant brain. NeuroReport, 1998, 9: 1885-1888.

Deouell, L.Y., Bentin, S. and Giard, M-H. Mismatch negativity in dichotic listening: evidence for inter-hemispheric differences and multiple generators. Psychophysiology, 1998, 35: 355-365.

Escera, C., Yago, E., Polo, M.D. and Grau, C. The individual replicability of mismatch negativity at short and long inter-stimulus intervals. Clin. Neurophysiol., 2000, 111: 546-551.

Frodl-Bauch, T., Kathmann, N., Möller, H-J. and Hegerl, U. Dipole localization and test-retest reliability of frequency and duration mismatch negativity generator processes. Brain Topogr., 1997, 10: 3-8.

Fujiwara, N., Nagamine, T., Imai, M., Tanaka, T. and Shibasaki, H. Role of the primary auditory cortex in auditory selective attention studied by whole-head magnometer. Cog Brain Res., 1998, 7: 99-109.

Garnero, L., Baillet, S. and Renault, B. Internal Software. LENA UPR 640, Paris, France, 1998.

Giard, M-H., Perrin, F., Pernier, J. and Bouchet, P. Brain generators implicated in the processing of auditory stimulus deviance: a topographic event-related potential study. Psychophysiology, 1990, 27: 627-640.

Giard, M-H., Lavaikainen, J., Reinikainen, K., Perrin, F., Bertrand, O., Pernier, J. and Näätänen, R. Separate representation of stimulus frequency, intensity and duration in auditory sensory memory: an event-related potential and dipole-model analysis. J. Cogn. Neurosci.,1995, 7: 133-143.

Hillyard, S.A., Hinrichs, H., Tempelmann, C., Morgan, S.T., Hansen, J.C., Scheich, H., and Heinze, H-J.. Combining steady-state visual evoked potentials and fMRI to localize brain activity during selective attention. Human Brain Mapping, 1997, 5: 287-292.

Huotilainen, M., Winkler, I., Alho, K., Escera, C., Virtanen, J., Ilmoniemi, R.J.,

Jääskeläinen, I.P., Pekkonen, E. and Näätänen, R. Combined mapping of human auditory EEG and MEG responses. Electroencephalogr. Clin. Neurophysiol., 1998, 108: 370-379.

Javitt, D.C., Grochowski, S., Shelley, A-M. and Ritter, W. Impaired mismatch negativity (MMN) generation in schizophrenia as a function of stimulus deviance, probability and interstimulus/interdeviant interval. Electroencephalogr. Clin. Neurophysiol., 1998, 108: 143-153.

Jemel, B., Achenbach, C., Wiemer, P., Röpcke, B., and Oades, R.D. Auditory frequency- and duration-deviant detection elicit similar asymmetrical dipole sources localised in both the temporal lobe and in the frontal cortices. Neuroimage, 2001, 13: 323.

Joutsiniemi, S-L., Ilvonen, T., Sinkkonen, J., Huotilainen, M., Tervaniemi, M., Lehtokoski, A., Rinne, T. and Näätänen R. The mismatch negativity for duration decrement of auditory stimuli in healthy subjects. Electroencephalogr. Clin. Neurophysiol. 1998, 108:154-159

Karayanidis, F., Andrews, S., Ward, P.B. and Michie, P.T. ERP indices of auditory selective attention in aging and Parkinson's disease. Psychophysiology, 1995, 32: 335-350.

Kathmann, N., Frodl-Bauch, T. and Hegerl, U. Stability of the mismatch negativity under different stimulus and attention conditions. Clin. Neurophysiol., 1999, 110: 317-323.

Kathmann, N., Wagner, M., Rendtorff, N. and Engel, R.R. Delayed peak latency of the mismatch negativity in schizophrenics and alcoholics. Biol. Psychiatry, 1995, 37: 754-757.

Kiehl, K.A., Laurens, K.R., Duty, T.L., Forster, B.B. and Liddle, P.F. Neural sources involved in auditory target detection and novelty processing: an event-related fMRI study. Psycho-physiology, 2001, 38: 133-142.

Korzyukov, O., Alho, K., Kujala, A., Gumenyuk, V., Ilmoniemi, R.J., Virtanen, J., Kropotov, J. and Näätänen, R. Electromagnetic responses of the human auditory cortex generated by sensory-memory based processing of tone-frequency changes. Neurosci. Lett., 1999, 276: 169-172.

Laarne, P.H., Tenhunen-Eskelinen, M.L., Hyttinen, J.K. and Eskola, H.J. Effect of EEG electrode density on dipole localization accuracy using two realistically shaped skull resistivity models. Brain Topogr., 2000, 12: 249-254.

Leonard, C.M., Puranik, C., Kuldau, J.M. and Lombardino, L.J. Normal variation in the frequency and location of human auditory cortex landmarks. Heschl's gyrus: Where is it? Cerebral Cortex, 1998, 8: 397-406.

Levänen, S., Ahonen, A., Hari, R., McEvoy, L. and Sams, M. Deviant auditory stimuli activate left and right auditory cortex differently. Cereb. Cortex, 1996, 6: 288-296.

Mesulam, M-M. From sensation to cognition. Brain, 1998 121:1013-1052

Michie, P., Budd, T.W., Todd, J., Rock, D., Wichmann, H., Box, J. and Jablensky, A.V. Duration and frequency mismatch negativity in schizophrenia. Clin. Neurophysiol., 2000, 111: 1054-1065.

Müller, R-A., Kleinhans, N. and Courchesne, E. Broca's area and the discrimination of frequency transitions: a functional MRI study. Brain and Language, 2001, 76: 70-76.

Näätänen, R. Mismatch negativity (MMN): perspectives for application. Int. J. Psychophysiology, 2000, 37: 3-10.

Nobre, A.C., Coull, J.T., Frith, C.D. and Mesulam, M-M. Orbitofrontal cortex is activated during breaches of expectation in tasks of visual attention. Nature Neurosci., 1999, 2:11-12

Nunez. P.L Electric fields of the brain. Oxford University Press, New York, 1981

Oades, R.D. and Dittmann-Balcar, A. Mismatch negativity (MMN) is altered by directing attention. NeuroReport, 1995, 6: 1187-1190.

Oades, R.D., Dittmann-Balcar, A., Schepker, R., Eggers, C. and Zerbin, D. Event-related potentials (ERPs) responses to tones and mismatch negativity (MMN) in healthy children and those with attention deficit or Tourette/tic symptoms. Biol. Psychology, 1996a, 43: 163-185.

Oades, R.D., Zerbin, D., Dittmann-Balcar, A. and Eggers, C. The topography of event-related potentials and four subtraction waves in a three-tone auditory discrimination: young healthy adults and patients with obsessive-compulsive disorder, paranoid and non-paranoid psychosis. Int. J. Psychophysiology, 1996b,

22: 185-214.

Oades, R.D., Dittmann-Balcar, A., Zerbin, D. and Grzella, I. Impaired attention-dependent augmentation of MMN in nonparanoid vs. paranoid schizophrenic patients: a comparison with obsessive-compulsive disorder and healthy subjects Biol. Psychiatry, 1997, 41:1196-1210.

Opitz, B., Mecklinger, A., Friederici, A.D. and von Cramon, Y. The functional neuroanatomy of novelty processing: integrating ERP and fMRI results. Cerebral Cortex, 1999a, 9: 379-391.

Opitz, B., Mecklinger, A., von Cramon, Y. and Kruggel, F. Combining electro-physiological and hemodynamic measures of the auditory oddball. Psychophysiology, 1999b, 36: 142-147.

Otten, L.J., Alain, C. and Picton, T.W. Effects of visual attention on auditory processing. NeuroReport, 2000, 11: 875-880.

Pandya, D.N. Anatomy of the auditory cortex. Revue de Neurologie (Paris), 1995, 151: 486-494

Pasqual-Marqui, R.D. and Lehmann, D. Topographic maps, source localization, and the reference electrode: comments on a paper by Desmedt et al., Electroencephalogr. Clin. Neurophysiol., 1993, 88: 532-533.

Paus, T., Zatorre, R.J., Hofle, N., Caramanos, Z., Gotman, J., Petrides, M. and Evans, A.C. Time-related changes in neural systems underlying attention and arousal during performance of an auditory vigilance task. J. Cogn. Neurosci. 1997, 9: 392-408.

Paavilainen, P., Alho, K., Reinikainen, K., Sams, M. and Näätänen, R. Right hemisphere dominance of different mismatch negativities. Electroencephalogr. Clin. Neurophysiol. 1991, 78: 466-479.

Pekkonen, E., Jousmaki, V., Könönen, M., Reinikainen, K. and Partanen, J. Auditory sensory memory impairment in Alzheimer's disease: an event-related potential study. NeuroReport 1994, 5: 2537-2540.

Pekkonen, E., Rinne, T. and Näätänen, R. Variability and replicability of the mismatch negativity. Electroencephalogr. Clin. Neurophysiol. 1995, 96: 546-554.

Pernier, J., Perrin, F. and Bertrand, O. Scalp current density fields: concept and properties. Electroencephalogr. Clin. Neurophysiol., 1988, 69: 385-389.

Rempel-Clower, N.L. and Barbas, H. The laminar pattern of connections between prefrontal and anterior temporal cortices in the Rhesus monkey is related to cortical structure and function. Cerebral Cortex, 2000, 10: 851-865.

Rinne, T., Alho, K., Ilmoniemi, R.J., Virtanen, J. and Näätänen, R. Separate time behaviors of the temp-oral and frontal mismatch negativity sources. Neuroimage, 2000, 12: 14-19.

Sams, M., Kaukoranta, E., Hamalainen, M. and Näätänen, R. Cortical activity elicited by changes in auditory stimuli: different sources for the magnetic N100m and mismatch responses. Psychophysiology, 1991, 28: 21-28.

Scherg, M. and Berg, P. Use of a priori knowledge in brain electromagnetic brain activity. Brain Topogr., 1991, 4: 143-150.

Scherg, M. and Picton, T.W. Separation and identification of event-related brain potential components by brain electric source analysis. Electroencephalogr. Clin. Neurophysiol. Suppl. 1991, 42: 24-37.

Scherg, M., Vajsar, J. and Picton, T.W. A source analysis of the human auditory evoked potential. J. Cogn. Neurosci., 1989, 1:336-355.

Shelley, A-M., Silipo, G. and Javitt, D.C. Diminished responsiveness of ERPs in schizophrenic subjects to changes in auditory stimulation parameters: implications for theories of cortical dysfunction. Schizophr. Res., 1999, 37: 65-79.

Strange, B.A., Henson, R.N.A., Friston, K.J. and Dolan, R.J. Brain mechanisms for detecting perceptual, semantic and emotional deviance. Neuroimage, 2000, 12:425-433.

Talairach, J. and Tournoux, P. Co-Planar Stereotaxic Atlas of the human brain. Translated by M Rayport, Stuttgart: Georg Thieve Verlag, 1988.

Teale. P., Retile, M., Rojas, D.C., Sheeder, J. and Arciniegas, D. Fine structure of the auditory M100 in schizophrenia and schizoaffective disorder. Biol. Psychiatry, 2000, 48, 1109-1112.

Tervaniemi, M., Schröger, E., Saher, M. and Näätänen, R. Effects of spectral complexity and sound duration on automatic complex-

sound pitch processing in humans – a mismatch negativity study. Neurosci. Lett., 2000, 290: 66-70.

Tervaniemi, M., Lehtokoski, M., Sinkkonen, A., Virtanen, J., Ilmoniemi, R.J. and Näätänen, R. Test-retest reliability of mismatch negativity for duration, frequency and intensity changes. Clin. Neurophysiol. 1999, 110: 1388-1393.

Tiitinen, H., Alho, K., Huotilainen, M., Ilmoniemi, R.J., Simola, J. and Näätänen, R. Tonotopic auditory cortex and the magnetoencephalographic (MEG) equivalent of the mismatch negativity. Psychophysiology, 1993, 30: 537-540.

Waberski, T.D., Kreitschmann-Andermahr, I., Kawohl, W., Darvas, F., Ryang, Y., Gonnele, R., and Buchner, H. Spatio-temporal source imaging reveals subcomponents of the human auditory mismatch negativity in the cingulum and right inferior temporal gyrus. Neurosci. Lett., 2001, 308: 107-110.

Woods, D.L., Knight, R.T. and Scabini, D. Anatomical substrates of auditory selective attention: behavioral and electrophysiological effects of posterior association cortex lesions, Cog. Brain Res., 1994, 1: 227-240.

Yoshiura, T., Zhong, J., Shibata, D.K., Kwok, W.E., Shrier, D.A and Numagichi, Y. Functional MRI study of auditory and visual oddball tasks. NeuroReport, 1999, 10: 1683-1688.

Yvert, B., Bertrand, O., Thevenet, M., Echallier, J.F. and Pernier, J. A systematic evaluation of the spherical model accuracy in EEG dipole localization. Electroencephalogr. Clin. Neurophysiol. 1997, 102: 452-459.